Location-free Indoor Radio Map Estimation using Transfer learning

R. Jaiswal, M. Elnourani, S. Deshmukh, B. Baltasar Lozano

Abstract: Accurate estimation of radio maps is important for various applications of wireless communications, such as network planning, and resource allocation. To learn accurate radio map models, one needs to have accurate knowledge of transmitter and receiver locations. However, it is difficult to obtain accurate locations in practice, especially, in scenarios having a high degree of wireless multi-path. Alternatively, time of arrival (ToA) features, which are easier to obtain, can be employed for estimating radio maps. To this end, this paper investigates the application of the transfer learning method using ToA features for estimating radio maps under indoor wireless communications. The performance is compared with the scenarios where only the locations of receivers and both ToAs and locations of receivers, are used for estimating radio maps, assuming that locations are known. Due to the changes in propagation characteristics, a radio map model learned in a specific wireless environment cannot be directly employed in a new wireless environment. To address this issue, a data-driven transfer learning method is designed that transfers and fine-tunes a deep neural network model learned for a radio map from a source wireless environment to other distinct (target) wireless environments. Our proposed method predicts the training data required in the new wireless environments using a data-driven similarity measure. Our results demonstrate that using ToA (location-free) features results in superior performance for estimating radio maps in terms of the necessary number of sensor measurements for estimating radio maps with good accuracy, as compared to a location-based approach, where it may be difficult to have accurate location estimations. It leads to a saving of 70-90% of the necessary sensor measurement data for a mean square error (MSE) of 0.004.

C.1 Introduction

Estimating accurate radio maps is crucial for numerous applications in wireless communications, such as network planning, spectrum management, channel modelling, and resource allocation, to name a few. Radio maps provide typically the value of received power at every spatial location over a certain frequency band of interest in any geographical area. The received powers at distinct spatial locations vary due to distinct factors, for instance, reflections, diffractions, propagation loss, and objects that block the line of sight between a transmitter (Tx) and a receiver (Rx).

Most of the algorithms to estimate radio maps are based on the knowledge of the Tx and Rx locations. This is known as the location-based radio map estimation [34]. However, accurate knowledge of sensor locations is difficult to obtain specially in environments where high wireless multipath fading is present. Alternatively, one can employ the features based on the received signals, such as the time of arrival[1] (ToA) for estimating the radio maps. This is known as the location-free radio map estimation [6]. Both the location-based and the location-free features are combined to estimate the channel gain maps in [80].

Because of the differences in propagation characteristics, a radio map model developed in a specific wireless environment, may not work appropriately in the new wireless environments. Training of machine learning (ML) methods, as a consequence, require substantial data for new wireless environments. Thus, one needs to have a large number of samples and training epochs for training the deep neural network (DNN)-based methods. Moreover, adequate computational time and data acquisition cost are needed while training the DNN for each new wireless environment. For alleviating these costs, one can develop a radio map model in one wireless environment (source environment) and then smartly use this model in a similar wireless environment (target environment), by exploiting the concept of transfer learning (TL) [19].

Model-based transfer learning [19] is the process of exploiting acquired knowledge from a certain learning task to another target task. TL handles the issue of data scarcity in the target environment in terms of reducing the amount of necessary data for efficient learning. In the scenario of estimating radio maps, one may have learned a radio map model in one indoor wireless environment but needs to estimate radio maps in other similar indoor wireless environments. Using TL, one does not require to learn a solution from the very beginning in the target environment, which requires in general a large amount of data, instead, the knowledge from the source model can be exploited.

Few works consider exploiting TL for wireless communications. A TL-based approach has been employed from the perfect channel state information (CSI) scenario to the imperfect CSI scenario in underlay D2D communications for jointly allocating channel and power [36]. An estimation of radio maps for indoor wireless environments employing the locations of Txs and Rxs, using TL, is investigated in [34]. In [20], a model-based TL is employed for capturing the diversity of cellular traffic patterns of different cities. For improving the robustness of the spectrum sensing algorithm developed for cognitive radio, TL is also applied in [21]. For tackling the non-convex resource allocation problem in [32], TL is employed to transfer from one solver to another solver. In [23], the optimal transport-based TL approach is designed which minimises the Wasserstein distance [24] for wireless fingerprinting

[1]Time of arrival (ToA) is the time at which the radio signals arrive at the Rx from the Tx.

localization.

This work employs TL for estimating radio maps in indoor wireless communications environments when the wireless environment changes. The following are the key contributions of this paper:

- Design of an efficient DNN-based model that learns a radio map for an indoor wireless environment. Additionally, the design of a data-driven TL method that transfers a DNN model for a radio map learned from a *source* baseline indoor wireless environment to another distinct *target* indoor wireless environment and further fine-tunes that DNN model.

- Design of a data-driven similarity measure model that maps the images of indoor wireless environments to the mean square error (MSE) that will be achieved for the estimated radio map in a new indoor wireless environment when performing the TL operation from a baseline (source) environment to a new (target) environment.

- Estimation of the amount of training data required for training in the new wireless environment, depending on a certain criterion of the MSE and the training epochs thresholds for estimating the radio maps, while executing the TL operation, employing the data-driven similarity measure that we design.

- Extensive testing of our algorithms using simulated data from the Remcom simulator [33]. Our simulation results demonstrate that employing only ToA (location-free) feature is better in estimating accurate radio maps when the location information is not accurately known.

- Numerically, we show that the proposed TL method employing only ToA (location-free) feature requires less amount of training data as compared to the location-based method [34]. It is also shown experimentally that a similarity measure based on the Wasserstein distance (WD), which is widely used in TL, is not applicable to our radio map application.

The remaining paper is organized as follows: Section C.2 explains the generation of distinct wireless environments for TL. The proposed radio map estimation method is introduced in Section C.3. Section C.4 discusses the numerical results. Section C.5 presents the conclusion.

C.2 Generation of Wireless Environments

The highly accurate and standard ray-tracing 3D ray model [41], calculated using Remcom [33], is employed to obtain power measurements for real indoor wireless environments. Along this line, Figure C.1 depicts an indoor environment which consists of a single floor with two rooms. For obtaining power measurements $\{P(x_i^r)\}$ at every Rx location $\{x_i^r\}$, a transmitter "Tx" is placed at one fixed location $\{x^t\}$, where i is the receiver location index. Also, several receivers are uniformly located.

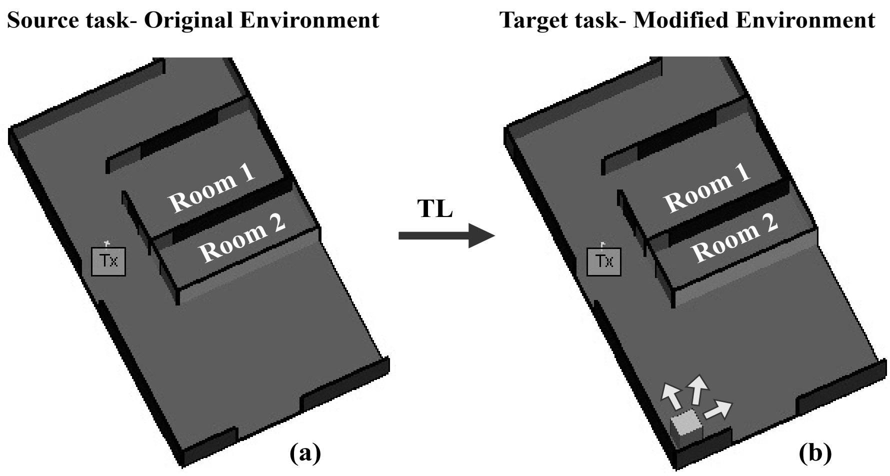

Figure C.1: TL environments: (a) original (source) environment, and (b) modified (target) environments.

Table C.1: Remcom parameters to generate data.

Waveform	Narrow-band Sinusoidal
Frequency of carrier with bandwidth	900 MHz (1 MHz)
Type of antenna	Omni-directional
Location of Tx	(1.5, 10, 1.3) m
Height of Tx	1.3 m
Power of Tx	27.73 dBm
Threshold of Receiver	-250 dBm
Voltage standing wave ratio (VSWR)	1.0
Loss of Transmission line	0 dB
Two Rx points separation	15 cm
Two Rx routes separation	15 cm
Noise figure	3 dB
Ray spacing	0.2°
No. of reflections, transmissions, and diffractions	3, 2, 0
Object volume (single cube)	1 m^3
Number of Rxs for locations and ToAs	6678
Dimension of floor (width x length x height)	(9.5 x 20.6 x 2.88) m
Total indoor environments generated	250
Floor image size (width x height)	(160 x 275) pixels

Similarly, for each Rx location $\{x_i^r\}$, we acquire the ToA estimated also using the model in [33], denoted as $\{\tau_i^r\}$, and we associate it with the corresponding received power at that location, which leads to a mapping of the form $\{P(\tau_i^r)\}$. The dimension of the floor, the sensor placement, and other parameters employed in Remcom are presented in Table C.1. A total of 6678 ToA features corresponding to every Rx location and power measurement are obtained.

Next, for creating distinct indoor wireless environments conceptually, an object, that is, a single solid cube block having a volume of $1m^3$ and made of metal is incorporated inside the original indoor environment. With an incremental spacing of 15cm, the location of the object changes in each direction, as depicted by arrows in Figure C.1(b). Each time new indoor environment generates whenever this object arrives at a new location. At the same time, the power measurements are obtained for this new environment by the ray-tracing model. This process results in 250 distinct indoor wireless environments. In addition, we save the images of each environment having an image size of 160 x 275 pixels. These images are later exploited for investigating different similarity measures for our TL problem, such as the WD and the data-driven similarity measure among distinct indoor wireless environments.

C.3 Radio Map Estimation Method

To estimate a radio map from a source to a target environment, the proposed TL scheme is depicted in Figure C.1. Defining similarity among source and target environments is important to perform TL operation. Along this line, a baseline DNN model (see Figure C.2) is developed in the source environment and then the target environment exploits this baseline model and fine-tunes it with additional data available from the target environment for establishing the similarity between both environments. In other words, the test MSE and the number of training epochs that are achieved after transferring the baseline DNN and re-training it in the new environments, are used as inputs to our data-driven similarity measure which is designed using the convolutional neural network (CNN) (see Figure C.3).

C.3.1 Baseline Model and TL Operation

Firstly, a DNN model is developed which approximates the power values for the original indoor environment (see Figure C.1(a)). Here we propose two methods. Method 1 uses both ToAs and locations of Rxs, and Method 2 uses only ToA (location-free) features. Along these lines, fully-connected DNN models are trained for each method and are referred to as respective “Baseline models”, as shown in Figure C.2.

Next, each baseline model is transferred to each new indoor environment (a total of 250 environments) and fine-tuned separately. Our hypothesis is: for training a DNN under the new environment, no ample amount of training data is available. Thus, to estimate radio maps in the new environment, one can exploit the TL operation for training a DNN model in the new environment with only a small amount of training data.

The data generated from Remcom (see Section C.2) is normalized to be between 0 and 1 to favour numerical stability in the training of DNN [34]. Let $\mathbf{P}(\tau_\mathbf{i}, \mathbf{x_i})$ and $\hat{\mathbf{P}}(\tau_\mathbf{i}, \mathbf{x_i})$ be the actual and the estimated power values, respectively, the mean

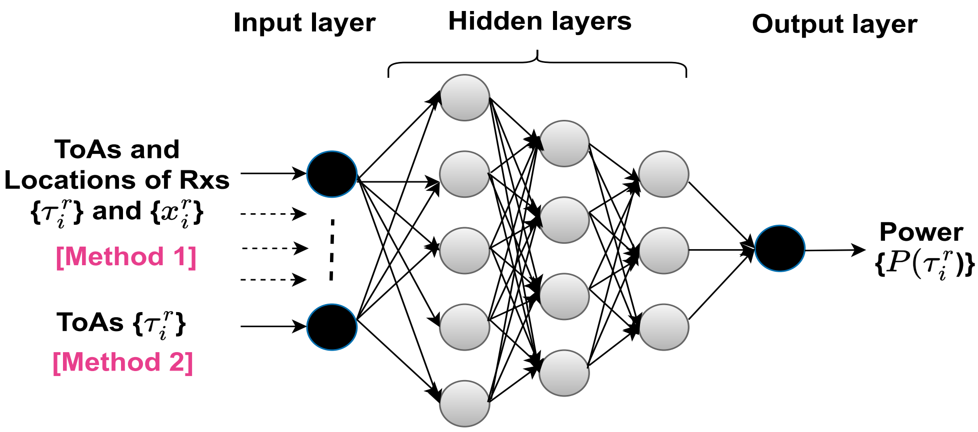

Figure C.2: DNN model for radio map estimation.

square error (MSE) [64] which is used as the loss function is calculated as, MSE = $\frac{\sum_{i=1}^{r}(\mathbf{P}(\tau_\mathbf{i},\mathbf{x_i})-\hat{\mathbf{P}}(\tau_\mathbf{i},\mathbf{x_i}))^\mathbf{2}}{r}$, where r is the total number of Rx locations.

Generally, the amount of training data needed for performing the TL operation relies on its similarity measure. For example, less amount of training data is needed between the two environments, if both environments are similar, and vice-versa. Thus, a similarity measure is needed to determine whether the TL operation is effective.

C.3.2 Similarity Measure based on the Wasserstein Distance

The Wasserstein distance (WD) [23] is one of the widely used similarity measures employed in the TL for establishing the similarity between a source and a target task. The distance between the two distributions is computed using WD. In the proposed TL scheme, the WD among the two images corresponding to the two different indoor wireless environments is computed. In practice, one computes cumulative distribution functions (CDFs) (see Equation C.1) empirically from the corresponding histograms with a sufficient amount of data. Let us consider two random variables S and T. In our case, S and T represent the image values corresponding to an environment in which the cube is located at the left bottom corner (see Figure C.1), and image values corresponding to another environment in which the cube is located at a distinct location, respectively. Let $F_S(s)$ and $F_T(t)$ be the respective CDFs. $\mathcal{F}_{ST}$ and $\mathbb{E}_{F_{ST}}[\cdot]$ be the joint CDFs, and the expectation with respect to the joint CDFs, respectively. The WD between both environments is calculated as [51]:

$$d(S,T) = \inf_{F_{ST}\in\mathcal{F}_{ST}} \mathbb{E}_{F_{ST}}[|S-T|] \tag{C.1}$$

C.3.3 Data-driven Similarity Measure

As shown later in Section C.4.2, it can be shown experimentally that typical similarity measures, such as the widely used WD, are not effective in our application of radio map estimation (as compared to other applications), since it is not able to track the variations of the radio maps as the indoor wireless environment varies.

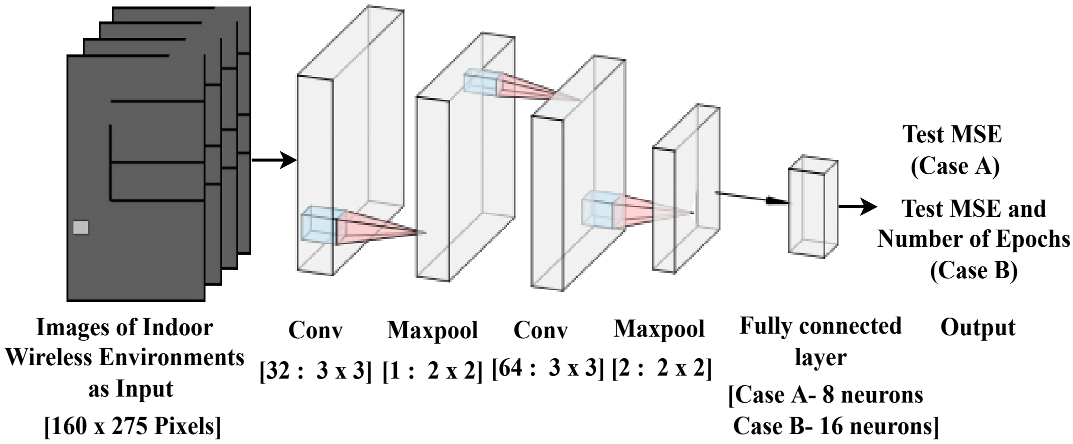

Figure C.3: CNN model for similarity measure.

This motivates the design of a data-driven similarity measure (DDS) for our TL problem that is able to understand the structure of the data in radio maps, and how it varies as the indoor wireless environment changes.

To determine the substantial reduction of training data during the TL operation using our data-driven similarity measure, the training data in the target indoor wireless environments varies from 5% to 40%. For establishing the similarity among the two environments, the test MSE corresponding to TL and the number of epochs employed in DNN training are stored, once the DNN is trained in each new (target) environment. Next, to design a DDS (see Figure C.3), a CNN regression model is trained within two distinct cases for each of the methods using both ToAs and locations of Rxs features, and using only ToA (location-free) features, respectively and then a threshold is set empirically for its comparison with the original one. The CNN networks used in both cases are shown in Figure C.3.

C.3.3.1 Case A

The images of distinct indoor wireless environments (a total of 250 environments) are the input of the CNN model. The test MSE obtained after performing the TL operation over each environment is the output of the CNN. Each coloured floor image has a size of 160 x 275 pixels. Before injecting these images into the CNN, they are converted into grayscale images using the OpenCV [81] library.

Next, for recommending the TL operation among two different environments, an empirical threshold for the test MSE corresponding to TL $\beta_{TestMSE}$ is set as 0.01. Two environments are recognized as sufficiently similar, if the test MSE obtained after performing the TL operation is less than this threshold, else, the TL operation is not recommended.

C.3.3.2 Case B

The same input (as in case A) is provided to the CNN model. The test MSE and the number of training epochs obtained after performing the TL operation over each environment are the output of the CNN model. The training epochs provide

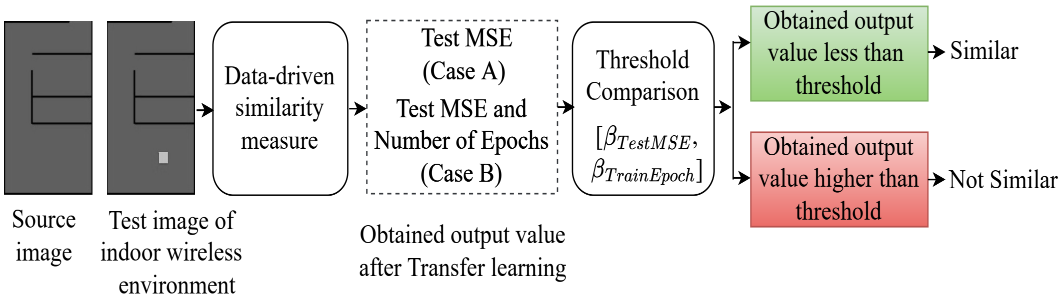

Figure C.4: Similarity decision between two wireless environments.

information about the time needed to train the model for a particular environment. Note that, a larger CNN model is required for this case, resulting in a need for larger feature sets. Hence, it becomes computationally demanding.

Next, for recommending the TL operation among two different environments, an empirical threshold for the test MSE corresponding to TL $\beta_{TestMSE}$, and the number of training epochs $\beta_{TrainEpoch}$ is set as 0.01 and 20, respectively. Two environments are recognized as sufficiently similar, if both values are less than these thresholds, else, the TL operation is not recommended. Figure C.4 illustrates the similarity decision taken between two indoor wireless environments under each case of the proposed TL method.

C.4 Results and Discussions

This section discusses the numerical results obtained in each method. Here we compare the performance of the proposed Method 1 and Method 2 with the TL method in [34] (Method 3) which employs only locations of Rxs for estimating radio maps in new indoor wireless environments.

C.4.1 Baseline DNN Model

Table C.2 presents the structures of the baseline DNN models that are used for each method (see Figure C.2). It also presents the structure of the baseline DNN model used in [34] which employs only locations of Rxs for estimating radio maps. We refer to the method used in [34] as *Method 3* for its comparison with Method 1 and Method 2. It can be seen from Table C.2 that under each method, the test MSE is comparable and is slightly larger than the train MSE which reflects no over-fitting in each baseline DNN model, resulting in successful learning of each baseline model.

Next, observe the test MSE obtained in Method 1 and Method 2 with the test MSE obtained in Method 3 in Table C.2, we notice that Method 1 and Method 2 have lesser test MSE values as compared to Method 3. Specifically, there is a reduction of around 69% and 55% in the test MSE values using both ToAs and Rx locations features (Method 1) and only ToA features (Method 2), respectively, as compared to using only locations of Rxs features (Method 3). This shows that Method 1 and Method 2 are having better baseline models as compared to Method 3 for the TL operation. Moreover, the test MSE of the baseline model under Method 2 (location-free) is almost the same as Method 1. Notice that the structure of each

Table C.2: The Baseline model learning

Parameters used	Both ToAs and locations of Rxs (Method 1)	Only ToAs (Method 2)	Only locations of Rxs [34] (Method 3)
Input layer neurons	4	2	2
Total hidden layers	6	3	2
Hidden layer neurons	512, 256, 128, 64, 32, 16	64, 32, 16	16, 8
Activation function in hidden layers	ReLU	ReLU	ReLU
Dropout after each hidden layer	-	-	0.20
Output layer neurons	1	1	1
Activation function in output layer	ReLU	ReLU	ReLU
Optimizer employed	Adam	Adam	Adam
Learning rate	0.0001	0.0001	0.001
Loss function	MSE	MSE	MSE
Size of mini-batch	16	16	32
Data split ratio for training-testing	70:30	70:30	80:20
Train MSE	0.00282	0.00459	0.0101
Test MSE	0.00313	0.00463	0.0102

baseline model in Table C.2 is optimal and is obtained using the grid search with its evaluation through 5-fold cross-validation.

C.4.2 Wasserstein Distance as a Similarity Measure

To test whether WD is suitable for our TL application, the WD between the floor images of indoor environments and the WD between their associated sampled radio maps (power values) when the cube is located at the left bottom corner (see Figure C.1(b)), and the rest of the indoor environments (a total of 250 environments) when the cube is located at other distinct locations, are calculated. Next, we compute Pearson's correlation coefficient (PCC) [34], which is one of the popular metrics for calculating correlations [20] between both kinds of WDs (floor images and associated sampled radio maps) across the several considered environments, then the correlation obtained is 0.08 that reflects a very poor correlation. This indicates that WD cannot be employed as a similarity measure for the TL-based radio map estimation in indoor wireless communications. The reason is that the WD is not able to capture effectively the changes in the radio maps caused by the variations in the locations of the cube. Hence, our designed data-driven similarity measure is exploited further for the TL-based radio map estimation problem.

Table C.3: The CNN model under Case A of Method 1.

Number of available indoor environments	250
Floor image size (width x height)	160 x 275
Total convolutional layers	2
Filters in 1^{st} and 2^{nd} convolutional layer	32, 64
Size of filters	3 x 3
Max pooling layers	2
Filter/pool size	2 x 2
Strides under 1^{st} and 2^{nd} convolutional layer	2
Convolutional layer activation function	ReLU
Dropout after 2^{nd} max pooling layer	0.3
Output layer neurons of neural network	8
Output layer activation function	ReLU
Optimizer with learning rate	Adam (0.001)
Loss function	MSE
Size of mini-batch	16
Data split ratio for training-testing	80:20
Train MSE	0.01768
Test MSE	0.02790

Table C.4: The CNN model under Case B of Method 1.

Total output layer neurons of neural network	16
Remaining configurations are the same as in Table C.3.	
Train MSE	0.01256
Test MSE	0.02047

C.4.3 Data-driven Similarity Measure

C.4.3.1 Method 1

The model learnings of the CNN under case A and case B for the Method 1, respectively, are presented in Tables C.3 and C.4. Note that, the configurations to train the CNN in case B are the same as in case A, except for the output layer neurons which have now become 16 due to the combination of both the test MSE and the number of training epochs corresponding to TL. Both Tables reflect a proper training of CNN under each case, that is, the testing MSE is comparable and slightly larger than the training MSE.

C.4.3.2 Method 2

The model learnings of the CNN under case A and case B for the Method 2, respectively, are presented in Tables C.5 and C.6. Both Tables reflect the proper training of CNN under each case.

Next, as explained in Section C.3.3, the decisions of recommendation of TL oper-

Table C.5: The CNN model under Case A of Method 2.

All parameters and hyper-parameters are same as in Table C.3.	
Train MSE	0.02134
Test MSE	0.03223

Table C.6: The CNN model under Case B of Method 2.

Total output layer neurons of neural network	16
Remaining configurations are the same as in Table C.3.	
Train MSE	0.01420
Test MSE	0.02276

Table C.7: Performance of proposed TL method.

	ToAs and locations of Rxs (Method 1)		Only ToAs (Method 2)		Only locations of Rxs [34] (Method 3)	
	Case A (Only MSE)	Case B (MSE and Epochs)	Case A (Only MSE)	Case B (MSE and Epochs)	Case A (Only MSE)	Case B (MSE and Epochs)
Training data needed after TL	No. of Envs.	No. of Envs.	No. of Envs.	No. of Envs.	No. of Envs.	No. of Envs.
5%	250	184	208	78	-	-
10%	-	5	35	49	-	-
15%	-	11	7	11	-	-
20%	-	5	-	19	-	3
25%	-	8	-	6	-	31
30%	-	3	-	10	17	152
35%	-	1	-	3	206	31
40%	-	5	-	1	23	-
% of training data after TL	5%	5-40%	5-15%	5-40%	30-40%	20-35%

ations for both case A and case B of each Method are determined and are presented in Table C.7. It shows the number of indoor wireless environments that follow our proposed TL strategy and the corresponding amount of training data required after performing the TL operations. Table C.7 illustrates that under case A of Method 1, all 250 distinct environments achieve the threshold criteria and are therefore recommended for TL, with a need of only 5% training data. This accounts for 100% TL recommendation rate. In the same manner, under case B using Method 1, 222 out of 250 distinct environments achieve the threshold criteria and are therefore recommended for TL, with a need of only 5-40% training data. This accounts for 88.8% TL recommendation rate. On the other hand, under case A using Method 2, all 250 distinct environments achieve the threshold criteria and are therefore recommended for TL, with a need of only 5-15% training data. This accounts for 100% TL recommendation rate. In the same manner, under case B of Method 2, 177 out of 250 distinct environments achieve the threshold criteria and are therefore recommended for TL, with a need of only 5-40% training data. This accounts for 70.8% TL recommendation rate. The reason for having a lower TL recommendation rate under case B for both Method 1 and Method 2 is due to not having a better correlation between the training epochs and the test MSE obtained after TL operation for the similarity measure.

Furthermore, in Table C.7, we also compare the requirement of the percentage of training data after TL under each case of Method 1 and Method 2 with Method 3, we notice that the wireless environments under case A of Method 1 require only 5% training data as compared to 30-40% in Method 3, saving around 85% training data. Similarly, most of the wireless environments under case B of Method 1 require only 5% training data and the remaining few wireless environments require only 10-40% training data. This illustrates the saving of a large amount of training data as compared to Method 3, where the wireless environments mostly require 20-35% training data. In the same manner, the wireless environments under case A of Method 2 (location-free) require only 5-15% training data as compared to 30-40% in Method 3, saving around 65% training data. Similarly, most of the wireless environments under case B of Method 2 (location-free) require only 5-10% training data and the remaining wireless environments require only 15-40% training data. This again demonstrates performance improvement in terms of saving a large amount of training data as compared to Method 3. In addition, observe that the percentage of training data required after TL under each case of Method 2 (location-free) is almost the same as Method 1. The above observation highlights that the presence of a small number of sensor measurements in the new (target) indoor wireless environments is sufficient to effectively estimate radio maps for Method 1 and Method 2.

C.4.4 Comparison of Reliability

To understand the reliability of the proposed TL method, transferability, F1-score and accuracy [69] are calculated for both cases under each Method. The effectiveness of the proposed method in recommending a correct TL is characterised by transferability. The model test accuracy is characterised by F1-score. All these measures range from 0 to 1. The higher values of these measures suggest that the developed model is better in respective performance.

To this line, Figure C.5 presents the transferability, F1-score and accuracy [69] for each case under each Method along with Method 3 for comparison. Notice that the transferability, F1-score and accuracy under case A of both Method 1 and Method 2 are higher than its corresponding case B. In addition, 100% accuracy is achieved by Method 1 and Method 2 under case A, which is higher than the corresponding value under case B. The reason for having lower accuracy under case B of both Method 1 and Method 2 is due to the small correlation between the training epochs and the test MSE obtained after TL operation for the similarity measure. Therefore,

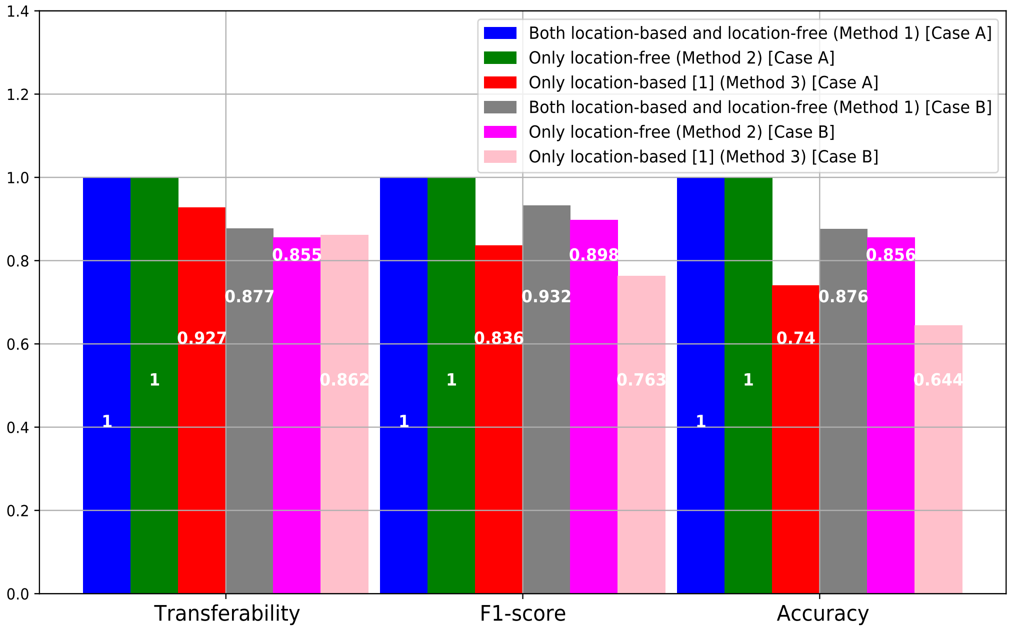

Figure C.5: Reliability comparison of different methods.

case A under both Method 1 and Method 2 performs better. On the other hand, the transferability, F1-score and accuracy under case B of Method 2 are slightly lower than the corresponding values under case B of Method 1.

Moreover, while comparing the transferability, F1-score and accuracy, in Figure C.5, under each case of Method 1 and Method 2 with Method 3, we notice that both cases under Method 1 and Method 2 are performing better than the corresponding cases under Method 3. In particular, there is an improvement of around 26% in accuracy under each case of Method 1 as compared to Method 3. Similarly, there is an improvement of around 24.5% in accuracy under each case of Method 2 (location-free) as compared to Method 3. In addition, the values of all measures under each case of Method 2 (location-free) are almost the same as Method 1.

Therefore, we can conclude from the results that the incorporation of ToA (location-free) features alone is satisfactory for estimating accurate radio maps in the new indoor wireless environments, which motivates using this method in scenarios with high wireless multi-path, where it may be difficult to have accurate location estimations.

C.4.5 Illustration of Radio Maps

We consider an indoor environment where the cube is present near the Tx. Figure C.6(b) shows the radio map for this environment without performing the TL operation. However, Figure C.6(c) and Figure C.6(d), respectively, illustrate the radio map for this same environment where only 40% of training data is needed while performing the TL operation using both ToA features and locations of Rxs (Method 1) and using only ToA features (Method 2). The solid black and dashed red colour, respectively, represent the cube and the walls of the rooms in the radio maps. It is clearly visible that the radio map estimated using only ToA features

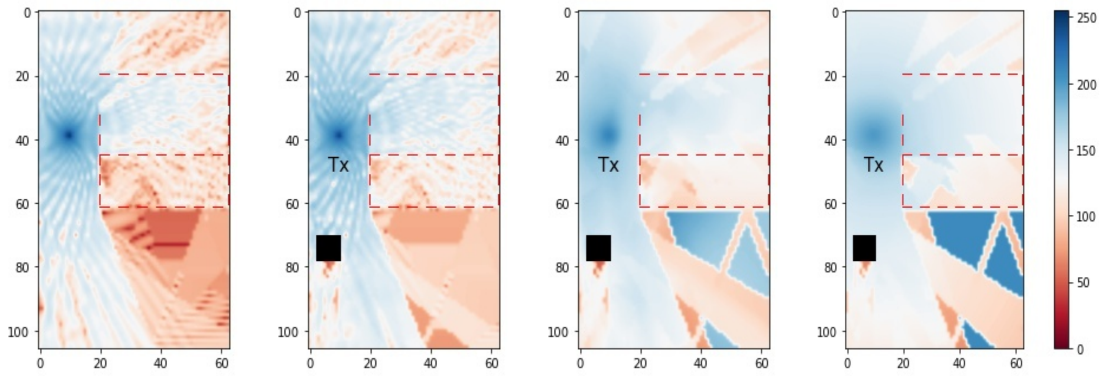

(a) (b) (c) (d)

Figure C.6: Radio map for (a) original indoor wireless environment, (b) a modified indoor wireless environment where the cube is present near the Tx, (c) same environment of (b) after executing the operation of TL using both ToA features and locations of Rxs (Method 1), where only 40% of training data is used for training the DNN resulting in a test MSE after TL as 0.00203, and (d) same environment of (b) after executing the operation of TL using only ToA features (location-free) (Method 2), where only 40% of training data is used for training the DNN resulting in a test MSE after TL as 0.00368.

(location-free) (Method 2) is smoother and satisfactory. In fact, the corresponding test MSE is very similar to the one obtained when using both ToA features and locations of Rxs (Method 1).

C.5 Conclusion

A TL-based radio map estimation method for indoor wireless networks is presented in this paper. We first design a method (Method 1) where both ToA features and locations of Rxs are used, assuming that the exact locations of receivers are known. Then, we consider a method (Method 2) based only on the ToA features (location-free). Moreover, for establishing the similarity between two wireless environments, a data-driven similarity measure is developed. This similarity measure is later employed for making a decision regarding the recommendation to perform TL operation, given only the image of the new wireless environment. Additionally, the performance of Method 1 and Method 2 is also compared with Method 3 [34], which employs only the locations of receivers for estimating radio maps. Satisfactory performance is observed while employing only ToA features (location-free), which motivates using this method in scenarios with high wireless multi-path where it may be difficult to have accurate location estimations. The proposed TL method employing only ToA features (location-free) also significantly reduces the number of training samples as compared to the location-based method [34] in similar indoor wireless environments and hence, a large amount of sensor measurements are saved.